



HAL
open science

Development of a label-free electrochemical aptasensor based on diazonium electrodeposition: Application to cadmium detection in water

Selma Rabai, Messaoud Benounis, Gaëlle Catanante, Abdoullatif Baraket, Abdelhamid Errachid, Nicole Jaffrezic Renault, Jean Marty, Amina Rhouati

► To cite this version:

Selma Rabai, Messaoud Benounis, Gaëlle Catanante, Abdoullatif Baraket, Abdelhamid Errachid, et al.. Development of a label-free electrochemical aptasensor based on diazonium electrodeposition: Application to cadmium detection in water. *Analytical Biochemistry*, 2021, 612, pp.113956. 10.1016/j.ab.2020.113956 . hal-03140071

HAL Id: hal-03140071

<https://hal.science/hal-03140071>

Submitted on 17 Oct 2022

HAL is a multi-disciplinary open access archive for the deposit and dissemination of scientific research documents, whether they are published or not. The documents may come from teaching and research institutions in France or abroad, or from public or private research centers.

L'archive ouverte pluridisciplinaire **HAL**, est destinée au dépôt et à la diffusion de documents scientifiques de niveau recherche, publiés ou non, émanant des établissements d'enseignement et de recherche français ou étrangers, des laboratoires publics ou privés.



Distributed under a Creative Commons Attribution - NonCommercial 4.0 International License

1 **Development of a label-free electrochemical aptasensor based on diazonium**
2 **electrodeposition: Application to cadmium detection in water**

3 Selma Rabai¹, Messaoud Benounis¹, Gaëlle Catanante², Abdoullatif Baraket³, Abdelhamid
4 Errachid³, Nicole Jaffrezic- Renault³, Jean-Louis Marty² and Amina Rhouati^{2, 4*}

5 ¹Laboratory of Sensors, Instrumentations and Process (LCIP), University of Khenchela,
6 Khenchela, Algeria.

7 ²Laboratory of Biosensors, Analysis and Environment (BAE), University of Perpignan *Via*
8 *Domitia*, Perpignan, France.

9 ³Laboratory of Analytical Sciences, University of Claude Bernard 1, Doua 69100
10 Villeurbanne, Lyon, France.

11 ⁴Higher National School of Biotechnology, Constantine, Algeria.

12 *a.rhouati@ensbiotech.edu.dz

13 **Abstract:**

14 In this study we have developed a new aptasensor for cadmium (Cd^{2+}) detection in water. Gold
15 electrode surface has been chemically modified by electrochemical reduction of diazonium salt (CMA) with
16 carboxylic acid outward from the surface. This was used for amino-modified cadmium aptamer immobilization
17 through carbodiimide reaction. Chemical surface modification was characterized by cyclic voltammetry (CV)
18 and electrochemical impedance spectroscopy (EIS). This latter was also used for Cd^{2+} detection. The aptasensor
19 has exhibited a good linear relationship between the logarithm of the Cd^{2+} concentration and the impedance
20 changes in the range from 10^{-3} to 10^{-9} M with a correlation R^2 of 0.9954. A high sensitivity was obtained with a
21 low limit of detection (LOD) of 2.75×10^{-10} M. Moreover, the developed aptasensor showed a high selectivity
22 towards Cd^{2+} when compared to other interferences such as Hg^{2+} , Pb^{2+} and Zn^{2+} . The developed aptasensor
23 presents a simple and sensitive approach for Cd^{2+} detection in aqueous solutions with application for trace Cd^{2+}
24 detection in spring water samples.

25 **Keywords:** Label-free detection, aptasensor, diazonium electrografting, gold electrode, cadmium detection.

26 **Introduction**

27 Recently, pollution caused by heavy metals is becoming more and more severe. Heavy metals are
28 naturally occurring elements characterized by high atomic weight and density, which is at least five times greater
29 than that of water [1]. The distribution of heavy metals; like Arsenic, Cadmium, Chromium, Lead, and Mercury
30 in the environment is a result of their multiple applications, and raising concerns about their potential effects on
31 human health and environment in most regions around the world, because of their high degree of toxicity [2].
32 Cadmium (Cd^{2+}) is a toxic heavy metal whose presence in the environment is mainly issued from human
33 activities [3]. It is produced in the manufacture of batteries and pigments which can permeate, soil and water
34 supply. Thereby, exposing the general population to low Cd^{2+} doses can affect a variety of cellular mechanisms
35 such as proliferation, apoptosis, differentiation, cell signalling and gene expression. For these reasons,
36 Cadmium has been classified as carcinogenic to humans by the World Health Organization (WHO) even at low
37 doses, the maximum limit is $0.003 \text{ mg}\cdot\text{L}^{-1}$. Indeed, it has been reported that exposure to this ion plays a particular
38 role in prostate cancer[4, 5].[4]. Numerous analytical methods traditionally used for detection of Cadmium (II)
39 ions have been widely reviewed in the literature; like atomic absorption/emission spectroscopy (AAS/AES) [6,
40 7], ultraviolet-visible spectrometry [8], Square-wave anodic stripping voltammetry [9] and atomic fluorescence
41 spectrometry (AFS) [10]. Despite their performance, most of these methods are often tedious, time consuming
42 and require great amounts of solvents, reagents and sophisticated apparatus. Therefore, inexpensive, sensitive
43 and selective techniques are very desirable for cadmium monitoring.

44 Biosensors are considered as very promising tools for sensitive, rapid and low cost monitoring of wide
45 range of analytes in different fields of applications. A wide range of biomolecules or chemical species have been
46 used in the literature as sensitive layer for chemical or biosensors manufacturing[11]. Aptamers are considered
47 as bio-inspired receptors which have gained great interest since their discovery in 1990 [12].

48 Aptamers are RNA or DNA molecules with specific 3D structures, selected by *in vitro* selection process
49 called Systematic Evolution of Ligands by Exponential Enrichment (SELEX) [13]. Due to their unique
50 conformations, aptamers can bind a wide range of targets such as small molecules, proteins, and even whole
51 cells. Their advantageous characteristics, such as high stability, simple chemical synthesis, possibility of
52 modification, made them strong competitors of antibodies in molecular analysis [14-16]. They constitute thus

53 good candidates as effective probes for chemical sensors. Several aptasensors have been developed in the
54 literature for Cadmium ions detection. Hamid et al [17] have developed an electrochemical cadmium sensor
55 using a DNA aptamer, where the sensing mechanism was based on target binding-induced conformational
56 change. Here, magnetic beads were used as immobilization support for the aptamer. Despite the biosensor
57 selectivity toward Cd^{2+} , the detection range [250-1000 nM] of this electrochemical sensor was still rather
58 narrow. In another report, Guo et al. have developed a new colorimetric method for sensing Cd^{2+} by using
59 unmodified AuNPs [18]. Here, the linear detection range [5-40 μM] of this method was narrow and could not be
60 used for the detection of Cd^{2+} in various types of samples.

61 The critical point in aptasensor fabrication technology remains in the immobilization of active
62 biomolecules onto the transducer surface. Several immobilization techniques can be adopted according to the
63 biomolecules architecture and the desired application. For instance, direct attachment of bioreceptors to gold
64 electrodes has been reported, by using 3' or 5' thiol-labelled aptamers self-assembly through gold-sulfur bond
65 interaction by forming ordered single-carrier membrane [19, 20]. However, this technique suffers from non-
66 specific adsorption (random adsorption) and cannot be applied on other materials. Attachment of aptamers onto
67 sensor surfaces based on hybridization with partially complementary oligonucleotides has been also adopted
68 [20]. Nevertheless, annealing and hybridization steps are required, enduring thus the experimental conditions.
69 Covalent attachment to chemically-modified sensor surfaces is a promising method based on the interaction of a
70 labelling group and a chemically functionalized surface resulting in a layer of ordered film of aptamers.
71 Chemical covalent attachment may increase the specificity and selectivity of the aptasensing strategy [20].

72 In this study we have chosen an amino-modified aptamer for Cd^{2+} detection that we immobilized on
73 screen printed gold electrode through diazonium salt chemistry. To the best of our knowledge, this is the first
74 report describing an electrochemical aptasensor exploring diazonium-coupling reaction mechanism for Cd^{2+}
75 determination. To achieve that, Cd^{2+} aptamer was immobilized onto gold electrodes through 4-carboxymethyl
76 aryl diazonium (CMA) molecules which are electrochemically reduced on the electrode surface. Unlike
77 conventional grafting methods, diazonium salt-based electrochemical deposition involves simple reagents
78 without isolation and purification steps [21-24]. Gold working electrodes (WE) have been characterized with
79 cyclic voltammetry (CV) and electrochemical impedance spectroscopy (EIS) before and after WE chemical
80 surface modification and after aptamer immobilization. EIS was then used to monitor the extent of binding
81 between Cadmium and its specific capture aptamer.

82 **Experimental**

83 **Chemicals and Reagents**

84 Cadmium (II) nitrate [Cd (NO₃)₂], 4-aminophenylacetic acid (4-carboxymethylaniline CMA), Sodium nitrite
85 (NaNO₂), isopropyl alcohol (IPA) 96%, N-hydroxysuccinimide (NHS) and N-(3-dimethylaminopropyl)-N'-
86 ethyl-carbodiimide hydrochloride (EDC) were obtained from Sigma-Aldrich, France. Phosphate buffer
87 (NaH₂PO₄.H₂O ; Na₂HPO₄.2H₂O) and KCl solution containing ferricyanide K₃ [Fe(CN)₆] and ferrocyanide K₄
88 [Fe(CN)₆] were used as supporting electrolytes. Cadmium aptamer was synthesized and purchased by
89 Microsynth (Switzerland). The specific sequence of the aptamer was as follows: (5' amino-modified):5'-ACC
90 GAC CGT GCT GGA CTC TGG ACT GTT GTG GTA TTA TTT TTG GTT GTG CAG TAT GAG CGA GCG
91 TTG CG-3' [25].

92 **Electrochemical analysis**

93 The electrochemical experiments were carried out with a potentiostat (Biologic EC-Lab SP-300). The
94 electrochemical measurements were performed in PBS with pH 7.4 at room temperature in a conventional
95 electrochemical glass cell containing three-electrode system [26].

96 Cyclic Voltammetry (CV) measurements were used before and after chemical gold surface modifications. CV
97 analysis were performed in 5 mM of [Fe(CN)₆]^{3-/4-} solution within a potential range of (- 0.2V to + 0.6V) and a
98 scan rate of 80 mV.s⁻¹.

99 Electrochemical impedance spectroscopy (EIS) was used to study the barrier properties of the modified electrode
100 [27, 28]. The EIS measurements were conducted at a potential of 128 mV on the Gold WEs over a frequency
101 range between 100 mHz and 200 kHz. The data of EIS were fitted using Randles equivalent circuit model. The
102 modelling of the obtained EIS data was made by the EC-Lab software using the Randomize + Simplex method.
103 Here, randomize was stopped on 100 000 iterations and the fit stopped on 5000 iterations.

104 **Real sample analysis**

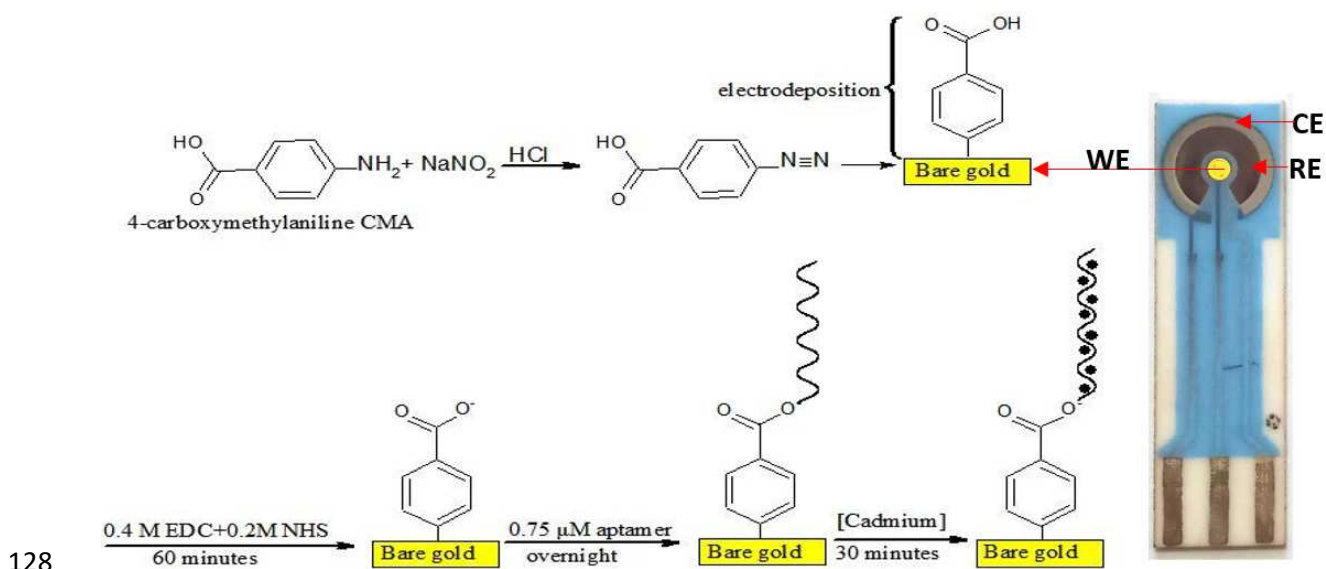
105 In order to validate and evaluate the accuracy and applicability of the our aptasensor, analyses were carried out
106 on a real river water which is polluted by public work wastes and containing nitrate and cadmium [29, 30]. This
107 river is crossed by a volcanic water source from Hammam Essalihine valley (khenchela, Algeria) which is rich in
108 minerals, such as bicarbonates, sulphates, calcium and magnesium. We have made sampling from the river

109 which contains cadmium and other potential interferences. Real samples were tested by EIS combined with
 110 standard addition method [31]. This method consists of adding known amounts of a standard solution to a
 111 sample of interest with unknown concentrations. Then, the analytical signals of standard solutions are recorded
 112 in response to each addition [31]. In brief, a constant volume (2.5mL) of water real sample was added to each
 113 flask of 25mL. Then in the first flask, a 22.5mL of PBS were added to the 2.5mL of real samples in order to
 114 reach a final volume of 25 mL and this flask was called **Level 1**. The standard solution containing the analyte
 115 was then added in increasing volumes: 0.25, 2.5 and 5 mL, implying the addition of 10, 100 and 200 nM of Cd²⁺
 116 to the subsequent flasks 2, 3 and 4. Finally these flasks were made up to the volume of 25 mL with PBS giving
 117 thus **Level 2, Level 3 and Level 4**, respectively.

118 **Results and discussion**

119 *Electrochemical aptasensor preparation*

120 Fig.1 illustrates the detection principle of Cd²⁺ by using the electrochemical aptasensor. Cd²⁺-aptamer
 121 immobilization was achieved through the covalent linkage between amino groups of the aptamer and the
 122 abundant reactive carboxylic groups on the gold surface. The electrode surface was first modified by deposition
 123 of a diazonium salt film, and activation of the terminal carboxylic groups with EDC/NHS. Then, the aptamer
 124 was linked to the gold surface via its activated carboxylic groups. In the presence of Cd²⁺, a variation in the
 125 aptamer conformation takes place from a random coil structure to an aptamer–Cd²⁺ complex [32, 33]. This
 126 aptamer-target interaction hampers the electron transfer, enhancing thus the surface resistance which is
 127 proportional to cadmium concentration in the sample.

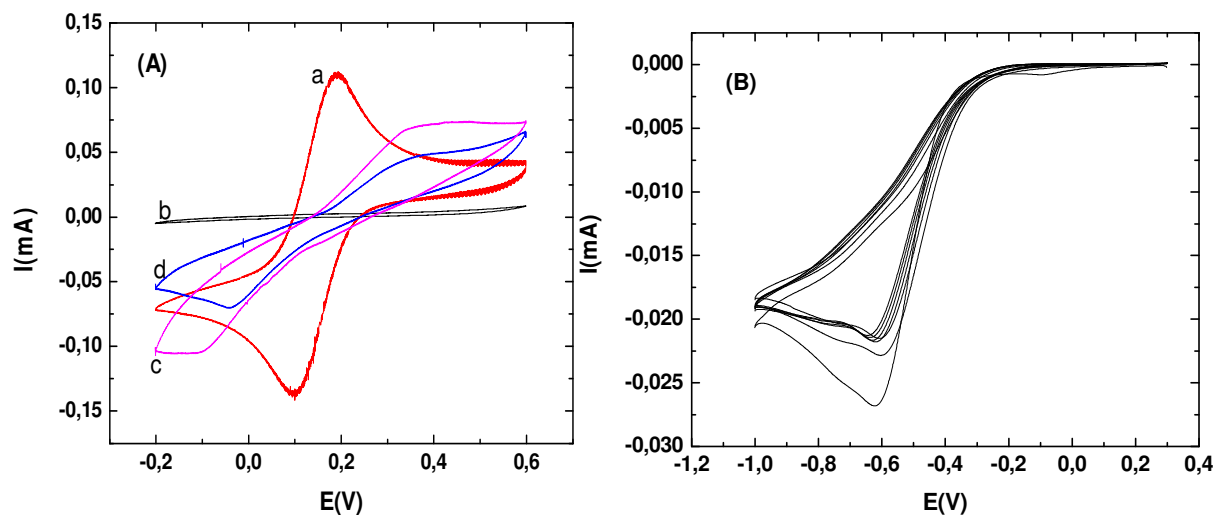


129 **Fig. 1** Schematic illustration of gold WE chemical surface modification by CMA followed by aptamer and
130 immobilization for Cadmium detection[32, 33]using integrated RE and CE.

131 **Characterization of the functionalized gold surface**

132 *Cyclic voltammetry studies*

133 For the Cyclic Voltammetry studies, **Fig.2A** shows the different cyclic voltammograms of the construction steps
134 of this aptasensor. The oxidation-reduction peaks of the redox couple are visible for the bare Gold WE. **Fig.2A**
135 **(a)** showing a pair of quasi-reversible peaks characteristic of the oxidation-reduction with cathodic and anodic
136 current peak ratio of approximately one and peak-to-peak separation of 0,1V. Then, a significant decrease in the
137 current **Fig.2A (b)** has been observed after the electrochemical grafting of diazonium salt **Fig.2B**. The
138 electrochemical reduction of the diazonium salt was generated *in situ* by a reaction of CMA with NaNO₂ in a
139 solution of HCl, with a scanning speed of 80 mV.s⁻¹, and within a potential range of (-0.2 to -1V). In the first
140 cycle, the current variation showed a reduction wave localized at -0.6V. This current corresponds to the
141 reduction of the diazonium salt in solution which leads to the formation of a radical amine. Afterwards, we
142 noticed from the second scan cycle that the reduction current decreases remarkably. This can be attributed to the
143 decrease of the electron transfer rate that was created by the CMA blocking layer. This was confirmed by a
144 significant decrease in the current **Fig.2A (b)**. After aptamer immobilization, CV peaks at the electrode have
145 significantly increased compared to CMA modified gold WE electrode **Fig.2A(c)**. This implies that most of the
146 surface of the electrode was covered with aptamer and demonstrates successful aptamer immobilization. Then,
147 the modified gold WE was incubated in a PBS solution containing 1nM cadmium Cd²⁺ during 30mn followed by
148 CV measurement **Fig.2A (d)**. Here we have again a decrease of CV peaks which means that the Cd²⁺ have been
149 successfully adsorbed onto the gold WE surface. The Cd²⁺ adsorption prevents or decreases the transfer of
150 electrons between gold WE surface and the redox couples in solution due to the opening of the rod portion of
151 aptamer and formation of the complex Cd²⁺- aptamer

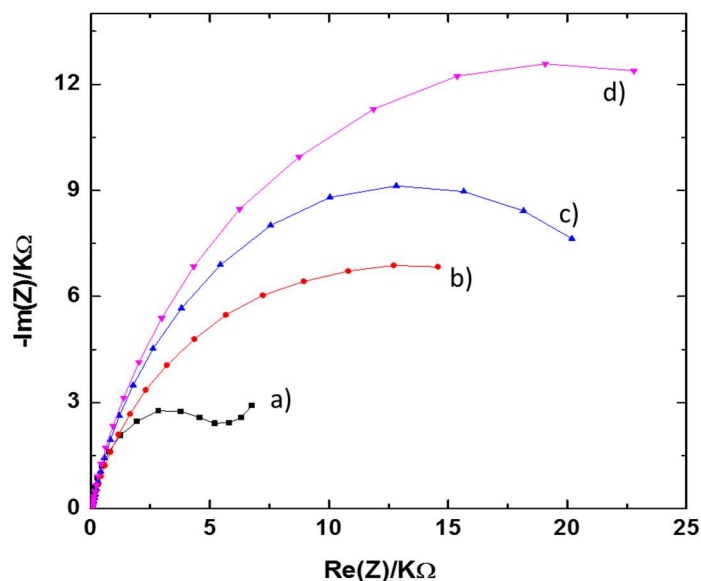


152

153 **Fig. 2** (A) Cyclic voltammograms of (a) bare gold WE (b) after CMA deposition (c) after aptamer immobilization
 154 and (d) after the detection for 10^{-9} M of Cd^{2+} solution. (B) Cyclic voltammograms for electrodeposition of CMA
 155 for repetitive potential cycles from -0.2 V to -1 V with a scan rate of $0.8 \text{ V} \cdot \text{s}^{-1}$
 156

157 **Electrochemical impedance spectroscopy studies**

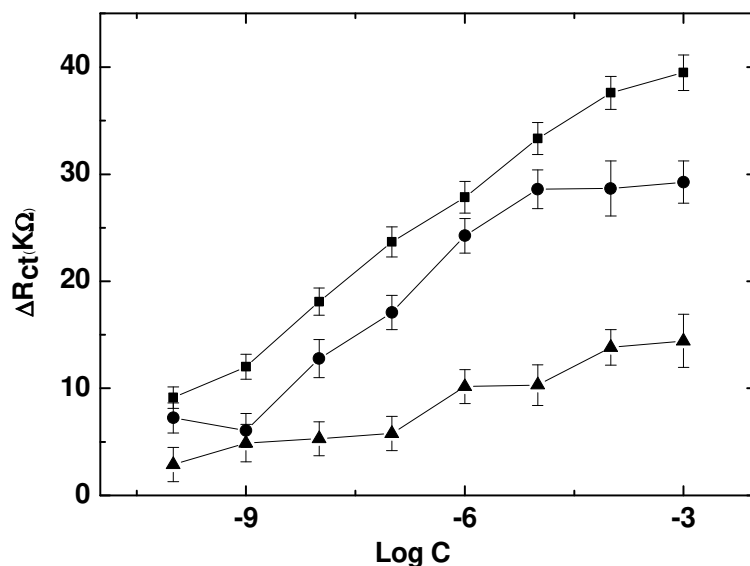
158 Impedance spectra were employed to assess the electrochemical behaviour of the aptasensor fabrication and
 159 realized in ferric potassium ferrocyanide solution. The Nyquist plot semi-circles allow to assess the transfer
 160 charge resistance R_{ct} generated by any modification on the gold WEs surface. The more the surface is passivated,
 161 the higher is the resistance R_{ct} value **Fig.3**. Here, the first Nyquist plot semi-circle **Fig.3 (a)** corresponds to the
 162 bare gold which presents negligible resistance R_{ct} . Then, the formation of an organic layer of CMA onto the gold
 163 WE surface has increased the R_{ct} to $25\,290 \, \Omega$ **Fig.3 (b)**. This was due to the CMA layer which decreases the
 164 electron transfer. Subsequently, the surface carboxylic groups were activated using carbodiimide chemistry to
 165 allow the Cd^{2+} -aptamer immobilization through the covalent linkage between amino groups of aptamer and the
 166 abundant reactive carboxylic groups of CMA. Aptamers immobilization has induced a strong increase in the
 167 semi-circular diameter, with an R_{ct} of $28\,096 \, \Omega$ **Fig. 3(c)**. Finally, the developed aptasensor was tested for
 168 Cadmium detection by incubating the aptasensor in Cd^{2+} solution at 10^{-9} M for 30 min. Here we observed an
 169 increase of R_{ct} up to $42\,537 \, \Omega$ **Fig.3(d)** due to the conformational changes induced by aptamer switching from a
 170 random coil structure to an aptamer–target complex [32, 33].



171 **Fig. 3:** Nyquist diagrams of the bare gold electrode (■), the electrochemically grafted CMA (●), after deposition
 172 of the aptamer (▲) and after incubation of Aptamer/CMA/AU in 10^{-9} M Cd^{2+} (▼) in the presence of 5 mM of
 173 $[\text{Fe}(\text{CN})_6]^{3-/4-}$ solution in a frequency range of 100 mHz - 200 kHz. The potential polarization used for these
 174 measurements was optimized at 128 mV.
 175

176 **Optimization of aptamer concentration**

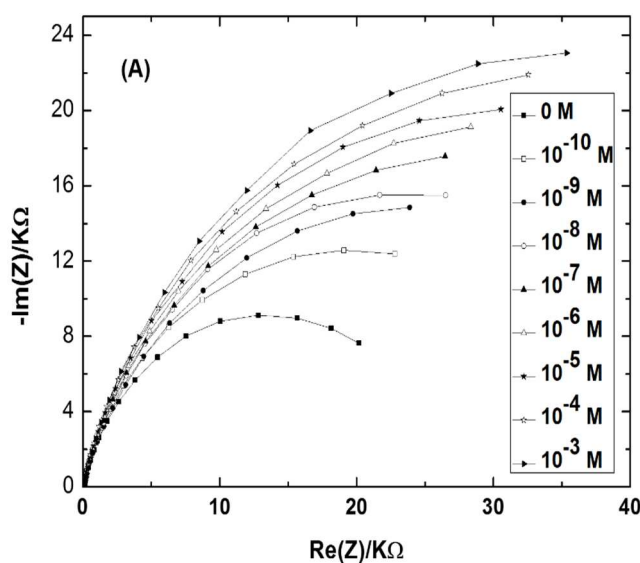
177 The aptamer concentration determines its final density onto the gold WE surface [34]. The optimization of
 178 aptamer concentration is a crucial step which affects the Cd^{2+} ions detection and the analytical performance of the
 179 aptasensor. Therefore, three different concentrations of aptamer (0.25, 0.5 and 0.75 μM) were tested within the
 180 range of 10^{-10} to 10^{-3} M of cadmium by using EIS. Fig. 4 shows the variation of R_{ct} as function of Cd^{2+}
 181 concentration for the three aptamer concentrations. As it can be observed, when using the aptamer concentration
 182 of 0.25 μM , the R_{ct} did not change significantly, to the weak complexation of the aptamer with its target. This
 183 aptamer concentration generated a low signal with a slope of 1.744 $\text{k}\Omega$ ($R^2= 0.927$). The aptamer concentration
 184 of 0,5 μM resulted a narrow range of linearity with a slope of 3.891 $\text{k}\Omega$ ($R^2=0.911$). Finally, by using the aptamer
 185 concentration of 0.75 μM , the signal was improved and the analytical response of the aptasensor was linear
 186 within the range of 10^{-9} to 10^{-4} M with a LOD of $2.75 \cdot 10^{-10}$ M. In addition, the sensitivity increased to 4.683 $\text{k}\Omega$
 187 when compared to that obtained with the lower concentrations.



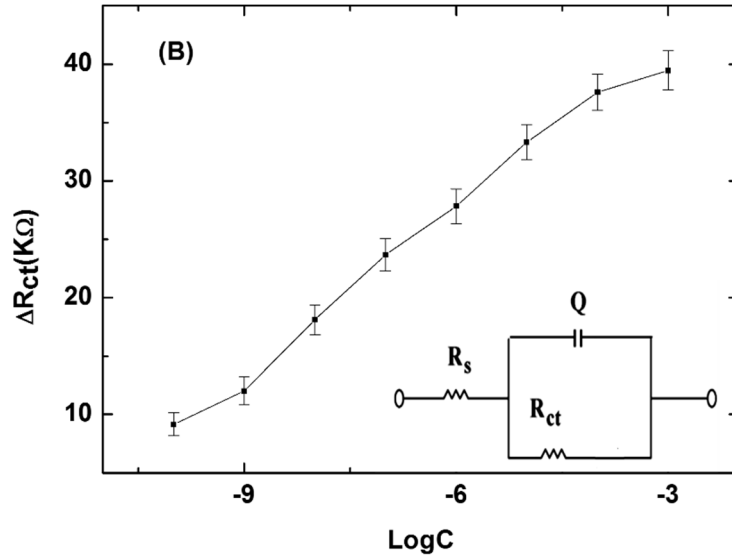
188 **Fig. 4** Optimization of Cd²⁺-aptamer concentration by EIS; (▲) 0.25 μM, (●) 0.5 μM and (■) 0.75 μM of
 189 aptamer.
 190

191 **Analytical performance of the aptasensor**

192 Under the optimal conditions, the aptasensor was used for cadmium detection in PBS buffer using EIS. To
 193 achieve that, the modified aptamer gold WE surface was incubated with different concentrations of cadmium for
 194 30 minutes. Experimental results showed a significant increase in the diameter of Nyquist plot semi-circles by
 195 increasing Cd²⁺ concentration **Fig. 5A**. The first Nyquist plot semi-circle corresponds to the aptamer-modified
 196 gold WE before the addition of cadmium. After incubation of aptasensor with increasing concentrations of the
 197 target, the Nyquist plot semi-circles continue to increase indicating the interaction between cadmium and its
 198 specific aptamer.



199



200

201 **Fig.5:** (A) Nyquist plots of Cd²⁺-aptamer-Gold WE surface incubated with increasing Cd²⁺ concentrations
 202 ranging from 10⁻³ to 10⁻¹⁰ M, (B) sensitivity of the aptasensor by normalization of the data towards the varying
 203 Cadmium concentrations. Inset: equivalent circuit used for the EIS Nyquist plot semi-circles fitting.

204

205

206

207

208

209

210

211

212

213

214

215

216

217

The transfer charge resistance R_{ct} was extracted from Nyquist plot semi-circles by using the equivalent circuit in Figure 5B Inset [21]. Where R_s represents the solution resistance, R_{ct} ; the charge-transfer resistance and Q ; the constant phase element (an equivalent model of double-layer capacitance). The real part of impedance ($Re(Z)$) increased as function of cadmium concentration. The linear regression equation was normalized to $\Delta R_{ct} = R_{ct}(\text{aptamer-cadmium}) - R_{ct}(\text{aptamer})$ as a function logarithm of Cadmium concentration. $R_{ct}(\text{aptamer-cadmium})$ is the value of the electron transfer resistance after Cd^{2+} binding to the immobilized aptamer on the modified electrode surface. $R_{ct}(\text{aptamer})$ represents the value of the electron transfer resistance after the aptamer immobilization on the CMA-modified electrode surface. The resistance of the aptasensor exhibited a linear correlation to Cadmium concentration through the range of (10⁻¹⁰-10⁻⁴M), with a good correlation coefficient of ($R^2 = 0.9954$) and a sensitivity of 4.683kΩ per cadmium concentration decade. The limit of detection (LOD) of the aptasensor is the concentration of cadmium corresponding to the 3 times “s/m” ratio, where “s” is the standard deviation of the blank impedance signal (three replicates) and “m” is the slope of the related calibration curve [35]. Here, the calculated LOD was 2.75*10⁻¹⁰M. The detection limit obtained in this work was lower the detection limits of Cd²⁺aptamer strategies and other methods (**Table 1**).

218

219

Table 1: Comparison of other sensors with different detection methods for the determination of Cd²⁺.

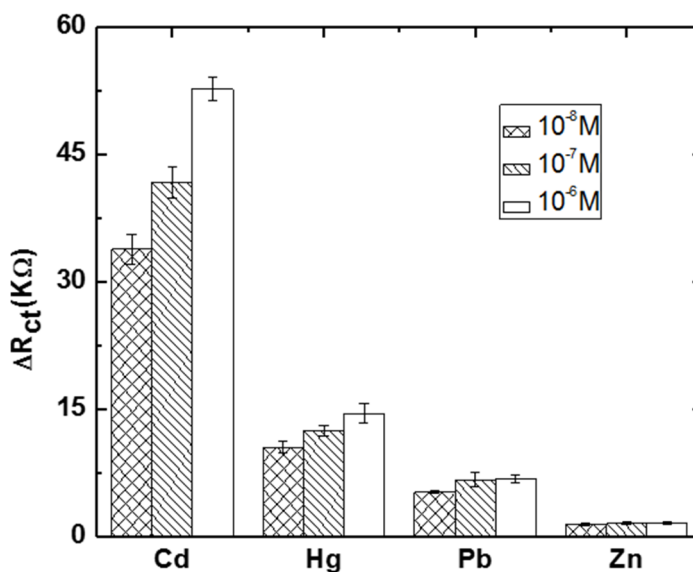
Detection methods	Linear range (nM)	Limit of detection (LOD) (nM)	Refs.
Fluorescent aptasensor	0 to 1000	40	[36]
Fluorescent aptasensor	7.19 to 200	2.15	[37]
Colorimetric aptasensor	10 to 400	4.6	[25]

Electrochemical aptasensor	1to1000	0.337	[38]
Electrochemical aptasensor	250 to 1000	92	[17]
Electrochemical aptasensor	0.1to10 ⁶	0.27	This work

220

221 The reproducibility of the developed aptasensor was tested with interassay precision. The interassay
 222 precision was evaluated by incubating three electrodes, independently prepared under the same experimental
 223 conditions with a same cadmium concentration of 10⁻⁶ M. A relative standard deviation from of 4.49% was
 224 calculated, indicating acceptable aptasensor reproducibility.

225 For the specificity study, the **Fig.6** depicts the impedance changes after incubation with Cd²⁺ and other
 226 heavy metals such as Hg²⁺, Pb²⁺ and Zn²⁺during 30 minutes. Three concentrations have been tested for each
 227 analyte; 10⁻⁸, 10⁻⁷ and 10⁻⁶M. At this stage, the interactivity of the aptasensor and cadmium detection was
 228 performed only in PBS buffer. As it can be observed in (Fig.6); the impedance responses show clearly that the
 229 aptasensor was highly selective to cadmium as compared to the other tested heavy metals. No significant signals
 230 have been recorded, even in the presence of Pb²⁺ and Zn²⁺. However, a slight cross-reactivity was noted with
 231 Hg²⁺,it may be attributed to the special T–Hg–T mismatched base pair between Hg²⁺ and Cd²⁺- aptamer[39-
 232 41].These results show that the selected aptamer immobilized on the electrode surface maintains its affinity and
 233 specificity in reaction with the cadmium, giving significant ΔR_{ct} increase. This may be considered as a
 234 validation of the proposed aptasensor selectivity, because it allows the discrimination between the tested heavy
 235 metals into the entire selected range.



236
 237
 238

Fig. 6 Selectivity studies of the aptasensor with Hg, Pb and Zn.

239 **Application in water samples by the standard addition method**

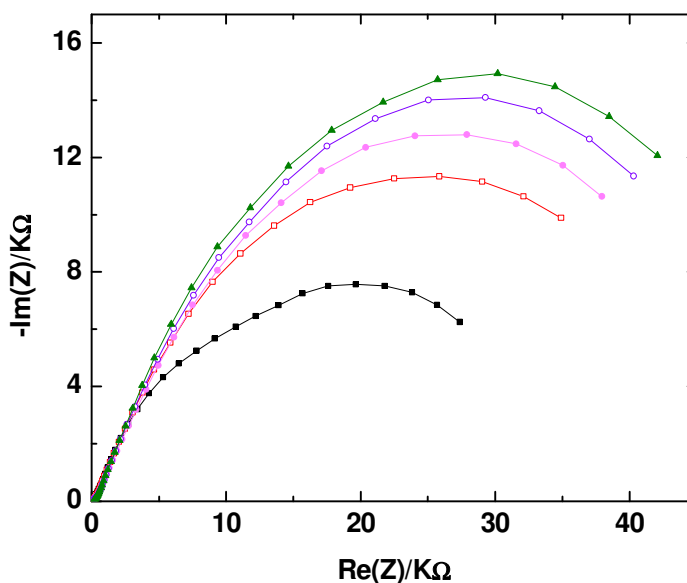
240 The developed aptasensor was applied for the detection of Cadmium in water samples of Hammam Essalihine
 241 valley using standard addition method as described previously. Four flasks containing the real water samples
 242 were prepared as mentioned in experimental, and then analysed by EIS measurements **Fig.7** depicts the first
 243 Nyquist plot corresponding to the aptamer-modified gold surface before cadmium addition, while the second one
 244 is attributed to the aptasensor after being incubated in the first flask (**level 1**) for 30 min. A shift in the semi-
 245 circle from the first one was observed, it was explained by the increase of resistance provided from aptamer
 246 reaction with cadmium. The second flask, corresponding to **level 2**, showed the same behaviour as the first flask.
 247 The analysis of the other flasks was performed in the same parameters. An increase in the semi-circular diameter
 248 was noticed and was absolutely explained by the increase of cadmium amount in the flasks. In order to determine
 249 the concentration of Cd²⁺ in the real sample, slope (m) and y-intercept (b) of the resulting calibration curve (R² =
 250 0.987) were used, and the unknown Cd²⁺ concentration of real sample was estimated to be 4.29.10⁻⁸M.

251 Table 2: Determination of Cd²⁺ by proposed aptasensors and atomic absorption spectroscopy (AAS) in water
 252 samples and recovery study of the aptasensor for determining cadmium

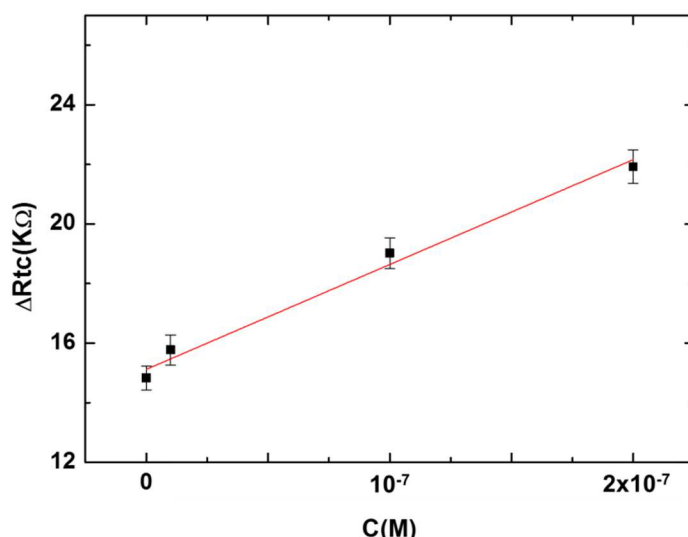
Ion in sample	AAS(C)	The aptasensor(Cs)	Recovery (%)
Cd ²⁺	4.76*10 ⁻⁸ M	4.29*10 ⁻⁸ M	90.12

253 $Recovery\% = C_s/C \times 100\%$ [42]

254 Aiming to validate our aptasensor, the tested sample was also analyzed by atomic adsorption
 255 spectroscopy (AAS) which is a reference method usually used for Cadmium detection[6, 7] . The obtained
 256 results are presented in (Table2). They are in a good agreement with those obtained by the standard addition
 257 method.



258



259

260 Fig. 7 (A) Nyquist impedance plots obtained from the performance application on a real sample. (■) PBS; (□)
 261 Level 1 (corresponding to an addition of 0 M); (●) Level 2 (addition of 10⁻⁸M); (○) Level 3 (addition of 10⁻⁷M)
 262 and (▲) Level 4 (addition of 2*10⁻⁷M). (B) Sensitivity curve used to calculate the concentration of analyte in the
 263 unknown sample by the standard addition method. Error bars represent the relative standard deviation on the
 264 measurements performed in triplicate.

265

266 Conclusion

267 In summary, we have developed an electrochemical aptasensor for Cadmium detection. The aptamer was
 268 covalently immobilized onto gold WE through CMA molecules. The studied aptasensor showed a linear
 269 relationship between the impedance changes and the logarithm of Cd²⁺ concentration in a broad range from 10⁻³
 270 to 10⁻¹⁰ M, with a LOD about 2.75*10⁻¹⁰M. Indeed, the present aptasensor displays excellent sensitivity and
 271 selectivity, in addition to a good reproducibility. Moreover, the aptasensor was highly selective to cadmium in
 272 the presence of other interferences, such as Hg²⁺, Pb²⁺ and Zn²⁺. In order to prove the method applicability, the
 273 constructed aptamer sensor has been employed to detect cadmium in real spring water samples with high
 274 accuracy. These promising results show that the developed method could be an excellent alternative for
 275 traditional techniques because of its accuracy, reliability, simplicity and low cost. This miniaturized sensor could
 276 be used wide wearable devices in rivers or directly in spring water sources. In addition, the working electrode
 277 could be functionalized by other aptamers to allow the concomitant determination of several heavy metals.

278 References

279 [1] S.J. Hawkes, What is a "heavy metal"?, Journal of Chemical Education, 74 (1997) 1374.
 280 [2] P.B. Tchounwou, C.G. Yedjou, A.K. Patlolla, D.J. Sutton, Heavy metal toxicity and the environment,
 281 Molecular, clinical and environmental toxicology, Springer 2012, pp. 133-164.

282 [3] A. Turner, Cadmium pigments in consumer products and their health risks, *Science of The Total*
283 *Environment*, (2018).

284 [4] D.G. Bostwick, H.B. Burke, D. Djakiew, S. Euling, S.m. Ho, J. Landolph, H. Morrison, B. Sonawane,
285 T. Shifflett, D.J. Waters, Human prostate cancer risk factors, *Cancer: Interdisciplinary International*
286 *Journal of the American Cancer Society*, 101 (2004) 2371-2490.

287 [5] F. Edition, Guidelines for drinking-water quality, *WHO chronicle*, 38 (2011) 104-108.

288 [6] N.A. Kasa, D.S. Chormey, Ç. Büyükpınar, F. Turak, T.B. Budak, S. Bakırdere, Determination of
289 cadmium at ultratrace levels by dispersive liquid-liquid microextraction and batch type hydride
290 generation atomic absorption spectrometry, *Microchemical Journal*, 133 (2017) 144-148.

291 [7] K.S. Rao, T. Balaji, T.P. Rao, Y. Babu, G. Naidu, Determination of iron, cobalt, nickel, manganese,
292 zinc, copper, cadmium and lead in human hair by inductively coupled plasma-atomic emission
293 spectrometry, *Spectrochimica Acta Part B: Atomic Spectroscopy*, 57 (2002) 1333-1338.

294 [8] D. Xu, W. Fan, H. Lv, Y. Liang, Y. Shan, G. Li, Z. Yang, L. Yu, Simultaneous determination of traces
295 amounts of cadmium, zinc, and cobalt based on UV-Vis spectrometry combined with wavelength
296 selection and partial least squares regression, *Spectrochimica Acta Part A: Molecular and*
297 *Biomolecular Spectroscopy*, 123 (2014) 430-435.

298 [9] L.C.S. Figueiredo-Filho, B.C. Janegitz, O. Fatibelilo-Filho, L.H. Marcolino-Junior, C.E. Banks,
299 Inexpensive and disposable copper mini-sensor modified with bismuth for lead and cadmium
300 determination using square-wave anodic stripping voltammetry, *Analytical Methods*, 5 (2013) 202-
301 207.

302 [10] Y.-k. Lü, H.-W. Sun, C.-G. Yuan, X.-P. Yan, Simultaneous determination of trace cadmium and
303 arsenic in biological samples by hydride generation-double channel atomic fluorescence
304 spectrometry, *Analytical chemistry*, 74 (2002) 1525-1529.

305 [11] H. Kaur, R. Kumar, J.N. Babu, S. Mittal, Advances in arsenic biosensor development—a
306 comprehensive review, *Biosensors and Bioelectronics*, 63 (2015) 533-545.

307 [12] C. Tuerk, L. Gold, Systematic evolution of ligands by exponential enrichment: RNA ligands to
308 bacteriophage T4 DNA polymerase, *science*, 249 (1990) 505-510.

309 [13] X. Sun, F. Li, G. Shen, J. Huang, X. Wang, Aptasensor based on the synergistic contributions of
310 chitosan-gold nanoparticles, graphene-gold nanoparticles and multi-walled carbon nanotubes-
311 cobalt phthalocyanine nanocomposites for kanamycin detection, *Analyst*, 139 (2014) 299-308.

312 [14] W. Tan, M.J. Donovan, J. Jiang, Aptamers from cell-based selection for bioanalytical applications,
313 *Chemical reviews*, 113 (2013) 2842-2862.

314 [15] K. Sefah, J. Phillips, C. Wu, Cell-Specific Aptamers for Disease Profiling and Cell Sorting,
315 *Aptamers Selected by Cell-SELEX for Theranostics*, Springer2015, pp. 197-213.

316 [16] K.-M. Song, S. Lee, C. Ban, Aptamers and their biological applications, *Sensors*, 12 (2012) 612-
317 631.

318 [17] H.R.L.Z. Zhad, Y.M.R. Torres, R.Y. Lai, A reagentless and reusable electrochemical aptamer-based
319 sensor for rapid detection of Cd (II), *Journal of Electroanalytical Chemistry*, 803 (2017) 89-94.

320 [18] Y. Guo, Y. Zhang, H. Shao, Z. Wang, X. Wang, X. Jiang, Label-free colorimetric detection of
321 cadmium ions in rice samples using gold nanoparticles, *Analytical chemistry*, 86 (2014) 8530-8534.

322 [19] I.M. Taylor, Z. Du, E.T. Bigelow, J.R. Eles, A.R. Horner, K.A. Catt, S.G. Weber, B.G. Jamieson, X.T.
323 Cui, Correction: Aptamer-functionalized neural recording electrodes for the direct measurement of
324 cocaine in vivo, *Journal of Materials Chemistry B*, 5 (2017) 8417-8417.

325 [20] Z. Ling, W. Ming-Hua, W. Jian-Ping, Y. Zhun-Zhong, Application of biosensor surface
326 immobilization methods for aptamer, *Chinese Journal of Analytical Chemistry*, 39 (2011) 432-438.

327 [21] A. Baraket, M. Lee, N. Zine, N. Yaakoubi, M.G. Trivella, M. Zabala, J. Bausells, N. Jaffrezic-Renault,
328 A. Errachid, Cytokine detection using diazonium modified gold microelectrodes onto polyimide
329 substrates with integrated Ag/AgCl reference electrode, 2012.

330 [22] L. Barhoumi, A. Baraket, F.G. Bellagambi, G.S. Karanasiou, M.B. Ali, D.I. Fotiadis, J. Bausells, N.
331 Zine, M. Sigaud, A. Errachid, A novel chronoamperometric immunosensor for rapid detection of TNF-
332 α in human saliva, *Sensors and Actuators B: Chemical*, 266 (2018) 477-484.

333 [23] A. Longo, A. Baraket, M. Vatteroni, N. Zine, J. Baussells, F. Di Francesco, G.S. Karanasiou, D.I.
334 Fotiadis, A. Menciacsi, A. Errachid, Highly sensitive Electrochemical BioMEMS for TNF- α detection in
335 humansaliva: Heart Failure, *Procedia Engineering*, 168 (2016) 97-100.

336 [24] S. Baranton, D. Bélanger, Electrochemical derivatization of carbon surface by reduction of in situ
337 generated diazonium cations, *The Journal of Physical Chemistry B*, 109 (2005) 24401-24410.

338 [25] Y. Wu, S. Zhan, L. Wang, P. Zhou, Selection of a DNA aptamer for cadmium detection based on
339 cationic polymer mediated aggregation of gold nanoparticles, *Analyst*, 139 (2014) 1550-1561.

340 [26] D.M. Jenkins, B. Chami, M. Kreuzer, G. Presting, A.M. Alvarez, B.Y. Liaw, Hybridization probe for
341 femtomolar quantification of selected nucleic acid sequences on a disposable electrode, *Analytical
342 chemistry*, 78 (2006) 2314-2318.

343 [27] A.B. Kharitonov, L. Alfonta, E. Katz, I. Willner, Probing of bioaffinity interactions at interfaces
344 using impedance spectroscopy and chronopotentiometry, *Journal of Electroanalytical Chemistry*, 487
345 (2000) 133-141.

346 [28] A. Hayat, L. Barthelmebs, A. Sassolas, J.-L. Marty, An electrochemical immunosensor based on
347 covalent immobilization of okadaic acid onto screen printed carbon electrode via diazotization-
348 coupling reaction, *Talanta*, 85 (2011) 513-518.

349 [29] H. Araar, M. Benounis, A. Direm, A. Touati, S. Atilia, H. Barhoumi, N. Jaffrezic-Renault, A new
350 thin film modified glassy carbon electrode based on melaminium chloride pentachlorocuprate (II) for
351 selective determination of nitrate in water, *Monatshefte für Chemie-Chemical Monthly*, 150 (2019)
352 1737-1744.

353 [30] K. Hanane, B. Messaoud, B. Houcine, T. Moncef, Highly sensitive modified glassy carbon sensor
354 based on TDAN for nitrate detection in real water, *Monatshefte für Chemie-Chemical Monthly*, 151
355 (2020) 153-158.

356 [31] F.G. Bellagambi, A. Baraket, A. Longo, M. Vatteroni, N. Zine, J. Bausells, R. Fuoco, F. Di Francesco,
357 P. Salvo, G.S. Karanasiou, Electrochemical biosensor platform for TNF- α cytokines detection in both
358 artificial and human saliva: Heart failure, *Sensors and Actuators B: Chemical*, 251 (2017) 1026-1033.

359 [32] Y. Luan, A. Lu, J. Chen, H. Fu, L. Xu, A label-free aptamer-based fluorescent assay for cadmium
360 detection, *Applied Sciences*, 6 (2016) 432.

361 [33] Z. Bagheryan, J.-B. Raoof, M. Golabi, A.P. Turner, V. Beni, Diazonium-based impedimetric
362 aptasensor for the rapid label-free detection of Salmonella typhimurium in food sample, *Biosensors
363 and Bioelectronics*, 80 (2016) 566-573.

364 [34] R.J. White, N. Phares, A.A. Lubin, Y. Xiao, K.W. Plaxco, Optimization of electrochemical aptamer-
365 based sensors via optimization of probe packing density and surface chemistry, *Langmuir*, 24 (2008)
366 10513-10518.

367 [35] C.M. Riley, T.W. Rosanske, *Development and validation of analytical methods*, Elsevier1996.

368 [36] H. Wang, H. Cheng, J. Wang, L. Xu, H. Chen, R. Pei, Selection and characterization of DNA
369 aptamers for the development of light-up biosensor to detect Cd (II), *Talanta*, 154 (2016) 498-503.

370 [37] Y.-F. Zhu, Y.-S. Wang, B. Zhou, J.-H. Yu, L.-L. Peng, Y.-Q. Huang, X.-J. Li, S.-H. Chen, X. Tang, X.-F.
371 Wang, A multifunctional fluorescent aptamer probe for highly sensitive and selective detection of
372 cadmium (II), *Analytical and bioanalytical chemistry*, 409 (2017) 4951-4958.

373 [38] X. Wang, W. Gao, W. Yan, P. Li, H. Zou, Z. Wei, W. Guan, Y. Ma, S. Wu, Y. Yu, A novel aptasensor
374 based on graphene/graphite carbon nitride nanocomposites for cadmium detection with high
375 selectivity and sensitivity, *ACS Applied Nano Materials*, 1 (2018) 2341-2346.

376 [39] C.-K. Chiang, C.-C. Huang, C.-W. Liu, H.-T. Chang, Oligonucleotide-based fluorescence probe for
377 sensitive and selective detection of mercury (II) in aqueous solution, *Analytical chemistry*, 80 (2008)
378 3716-3721.

379 [40] C. Gao, Q. Wang, F. Gao, F. Gao, A high-performance aptasensor for mercury (II) based on the
380 formation of a unique ternary structure of aptamer-Hg 2+—neutral red, *Chemical Communications*,
381 50 (2014) 9397-9400.

382 [41] C.-X. Tang, Y. Zhao, X.-W. He, X.-B. Yin, A “turn-on” electrochemiluminescent biosensor for
383 detecting Hg₂⁺ at femtomole level based on the intercalation of Ru (phen) 3₂⁺ into ds-DNA,
384 *Chemical Communications*, 46 (2010) 9022-9024.

385 [42] B. Dindar, E. Karakuş, F. Abasıyanık, New urea biosensor based on urease enzyme obtained from
386 *Helicobacter pylori*, *Applied biochemistry and biotechnology*, 165 (2011) 1308-1321.

387

388

389

390

